Francesco Endrizzi*, Xavier Gaona*, Zhicheng Zhang, Chao Xu, Linfeng Rao, Carmen Garcia-Perez and Marcus Altmaier

Thermodynamic description of U(VI) solubility and hydrolysis in dilute to concentrated NaCl solutions at $T = 25$, 55 and 80 °C

https://doi.org/10.1515/ract-2018-3056
Received September 4, 2018; accepted February 15, 2019

Abstract: The solubility and hydrolysis of U(VI) were investigated in 0.10–5.6 m NaCl solutions with $4 \le pH_m \le 14.3$ ($pH_m = -\log [H^+]$) at $T = 25$, 55 and 80 °C. Batch experiments were conducted under Ar atmosphere in the absence of carbonate. Solubility was studied from undersaturation conditions using $UO_3 \cdot 2H_2O$(cr) and $Na_2U_2O_7 \cdot H_2O$(cr) solid phases, equilibrated in acidic ($4 \le pH_m \le 6$) and alkaline ($8.2 \le pH_m \le 14.3$) NaCl solutions, respectively. Solid phases were previously tempered in solution at $T = 80$ °C to avoid changes in the crystallinity of the solid phase in the course of the solubility experiments. Starting materials and solid phases isolated at the end of the solubility experiments were characterized by powder XRD, SEM-EDS, TRLFS and quantitative chemical analysis. The enthalpy of dissolution of $Na_2U_2O_7 \cdot H_2O$(cr) at 25–80 °C was measured independently by means of solution-drop calorimetry. Solid phase characterization indicates the transformation of $UO_3 \cdot 2H_2O$(cr) into a sodium uranate-like phase with a molar ratio Na:U ≈ 0.4–0.5 in acidic solutions with [NaCl] ≥ 0.51 m at $T = 80$ °C. In contrast, $Na_2U_2O_7 \cdot H_2O$(cr) equilibrated in alkaline NaCl solutions remains unaltered within the investigated pH_m, NaCl concentration and temperature range. The solubility of $Na_2U_2O_7 \cdot H_2O$(cr) in the alkaline pH_m-range is noticeably enhanced at $T = 55$ and 80 °C relative to $T = 25$ °C. Combined results from solubility and calorimetric experiments indicate that this effect results from the increased acidity of water at elevated temperature, together with an enhanced hydrolysis of U(VI) and a minor contribution due to a decreased stability of $Na_2U_2O_7 \cdot H_2O$(cr) under these experimental conditions. A thermodynamic model describing the solubility and hydrolysis equilibria of U(VI) in alkaline solutions at $T = 25$–80 °C is developed, including $\log {}^*K^\circ_{s,0}\{Na_2U_2O_7 \cdot H_2O(cr)\}$, $\log {}^*\beta^\circ_{1,4}$ and related reaction enthalpies. The standard free energy and enthalpy of formation of $Na_2U_2O_7 \cdot H_2O$(cr) calculated from these data are also provided. These data can be implemented in thermodynamic databases and allow accurate solubility and speciation calculations for U(VI) in dilute to concentrated alkaline NaCl solutions in the temperature range $T = 25$–80 °C.

Keywords: Uranium(VI), solubility, hydrolysis, temperature, metaschoepite, sodium uranate, clarkeite, calorimetry, thermodynamics.

1 Introduction

Uranium is the main element present in spent nuclear fuel and accordingly contributes with the largest inventory to the High Level nuclear Waste (HLW) [1]. Although with a relatively minor contribution to the overall dose of the waste, uranium is the major component of the "matrix" embedding all other radionuclides in spent fuel, therefore requiring an accurate knowledge of the solution chemistry and solubility phenomena. Uranium is expected in the +IV redox state in the very reducing conditions foreseen in underground repositories. U(VI) prevails under mildly reducing to oxidizing conditions, although radiolysis effects can also promote the formation of U(VI) in the close vicinity of spent nuclear fuel even in the presence of H_2(g) [2]. In the absence of complexing ligands other than water/hydroxide, the hydrated uranyl oxide metaschoepite $UO_3 \cdot 2H_2O$(cr) and the uranates ($M_2U_2O_7 \cdot xH_2O$(cr), with M = Na, K, etc.) have been reported to control the solubility of U(VI) in acidic and alkaline pH conditions,

***Corresponding authors: Francesco Endrizzi and Xavier Gaona,** Karlsruhe Institute of Technology, Institute for Nuclear Waste Disposal, P.O. Box 3640, 76021 Karlsruhe, Germany,
E-mail: francesco.endrizzi@kit.edu (F. Endrizzi);
xavier.gaona@kit.edu (X. Gaona)
Zhicheng Zhang and Linfeng Rao: Lawrence Berkeley National Laboratory, Chemical Sciences Division, One Cyclotron Road, Berkeley, CA 94720, USA
Chao Xu: Institute of Nuclear and New Energy Technology, Tsinghua University, Beijing 100084, P.R. China
Carmen Garcia-Perez and Marcus Altmaier: Karlsruhe Institute of Technology, Institute for Nuclear Waste Disposal, P.O. Box 3640, 76021 Karlsruhe, Germany

respectively [3–7]. Elevated temperature conditions (up to 200 °C, depending on the host-rock system and repository concept) are expected to develop in the early stages of operation of repositories for HLW. In the event of early canister failure, aqueous systems may contact the waste and mobilize radionuclides outside the repository [2]. In this context, source term estimations (i. e. robust limiting values of the aqueous radionuclide concentration in the vicinity of the waste) are determined from the solubility limits using reliable experimental data and quality assured thermodynamic constants and parameters. Although thermodynamic data available for aqueous actinide systems at 25 °C are very extensive [8–11], dedicated solubility studies and thermodynamic data of actinide solid phases at elevated temperatures are instead very limited [12].

A critical review of the thermodynamic studies published until 2002/2003 for U, Np, Pu, Am and Tc was accomplished in the update book prepared within the thermochemical database (TDB) project of the Nuclear Energy Agency (NEA) [4]. Brown and Ekberg conducted a more recent review of the thermodynamic data available for the hydrolysis of metal ions, including uranium [13]. In a combined review and experimental work, Altmaier et al. comprehensively studied the solubility and hydrolysis of U(VI) at ambient temperature conditions [5]. Solubility experiments were performed from undersaturation conditions in 0.03–5.6 m (mol/kg of water) NaCl solutions at $T = 22$ °C. Metaschoepite, $UO_3 \cdot 2H_2O$(cr) was contacted with batch solutions equilibrating in the acidic pH_m range ($pH_m = -\log [H^+]$), while sodium uranate, $Na_2U_2O_7 \cdot H_2O$(cr) was used as starting material in experiments conducted in the neutral to alkaline pH_m range. Combining their experimental observations with potentiometric data available in the literature and using the NEA–TDB selection as anchoring point for hydrolysis constants of U(VI) species forming in acidic conditions, Altmaier and co-workers derived a comprehensive thermodynamic model for the system UO_2^{2+}–Na^+–H^+–Cl^-–OH^-–H_2O(l). The model included the solubility products of both solid phases, hydrolysis constants of U(VI) species forming in acidic to hyper-alkaline pH_m conditions and a set of empirical parameters to account for the effect of the ionic strength and specific-ion interactions, according to the SIT theory [4, 14]. In a later work, Endrizzi et al. extended the study of this system to elevated temperatures [15]. The solubility and hydrolysis equilibria of $UO_3 \cdot 2H_2O$(cr) and $Na_2U_2O_7 \cdot H_2O$(cr) were investigated in 0.51 m NaCl solutions at $T = 22$ and 80 °C. In contrast to the observations at $T = 22$ °C, a partial solid phase transformation of $UO_3 \cdot 2H_2O$(cr) into a sodium uranate-like solid phase was observed to occur already in acidic conditions, when the starting oxide was equilibrated in 0.51 m NaCl solutions at $T = 80$ °C. From the solubility data in the alkaline region a thermodynamic model was developed, including conditional solubility constants describing the dissolution of $Na_2U_2O_7 \cdot H_2O$(cr) under alkaline conditions, forming aqueous $UO_2(OH)_3^-$ and $UO_2(OH)_4^{2-}$ species predominant in solution (1):

$$0.5Na_2U_2O_7 \cdot H_2O(cr) + (x-2)H_2O(l) \leftrightarrow UO_2(OH)_x^{2-x} + Na^+ + (x-3)H^+ (x = 3,\ 4) \quad (1)$$

Results indicated that the solubility is not significantly impacted by temperature in the near-neutral region, while in the alkaline the solubility at $T = 80$ °C increases more than two orders of magnitude with respect to the one measured at $T = 22$ °C in the same electrolyte systems. This phenomenon is primarily attributed to the known increased acidity of water at elevated temperatures. An additional endothermic contribution is resulting from either a decreased stability of the solid phase and/or an enhanced stability of $UO_2(OH)_4^{2-}$ at higher temperatures. These two contributions could not be individually quantified, since only conditional solubility constants leading to the formation of $UO_2(OH)_3^-$ and $UO_2(OH)_4^{2-}$ ($\log {}^*K'_{s,(1,3)}$ and $\log {}^*K'_{s,(1,4)}$, (1) with $x = 3$ and 4, respectively) were obtained at this point. Although the solubility of $UO_3 \cdot 2H_2O$(cr) in acidic conditions and elevated temperatures was previously investigated in a number of studies [16–21], the work by Endrizzi et al. [15] is the only study available in the literature investigating the effect of temperature on the solubility of U(VI) in alkaline conditions.

As an extension of the solubility studies by Altmaier et al. [5] ($T = 22$ °C, 0.03–5.6 m NaCl) and Endrizzi et al. [15] ($T = 22$ and 80 °C, 0.51 m NaCl), this work presents a systematic thermodynamic study on the solubility and hydrolysis of $UO_3 \cdot 2H_2O$(cr) and $Na_2U_2O_7 \cdot H_2O$(cr) in 0.10, 0.51 and 5.6 m NaCl solutions at $T = 25$, 55 and 80 °C. The solubility study is complemented with a comprehensive solid phase characterization and the determination of the heat of dissolution of $Na_2U_2O_7 \cdot H_2O$(cr) by means of solution calorimetry. These data, in conjunction with $\log {}^*K'_{s,0}\{0.5Na_2U_2O_7 \cdot H_2O(cr)\}$ at $T = 25$ °C, are used to estimate the solubility constants at $T = 55$, 80 °C and to calculate $\Delta_f H_m^\circ$ and $\Delta_f G_m^\circ$ at $T = 25$ °C for this solid.

This work was conducted within the frame of the German collaborative project ThermAc. The goal of ThermAc is to improve and extend the understanding of the physicochemical processes and available thermodynamic database for actinides at elevated temperatures. The integrated concept in ThermAc includes as main strategic components (a) the systematic use of estimation

methods for thermodynamic data and model parameters, and (b) a comprehensive experimental validation for selected systems.

2 Experimental

2.1 Chemicals, synthesis and characterization of U(VI) solid phases

NaCl (p.a.), NaOH-Titrisol®, HCl-Titrisol® and Suprapur®-grade HNO_3 were purchased from Merck. $HClO_4$ (70 % solution in water, pur. >99.999 %) was obtained from Sigma-Aldrich. All solutions were prepared using Milli-Q deionized water (18.2 MΩ, Merck Millipore) and handled in an Ar-glovebox in conditions of exclusion of CO_2. Metaschoepite, $UO_3 \cdot 2H_2O$(cr) and sodium uranate ($Na_2U_2O_7 \cdot H_2O$(cr)) were prepared according to previous procedures [5] as follows: Metaschoepite, $UO_3 \cdot 2H_2O$(cr) was prepared in a argon, CO_2-free atmosphere by very slow dropwise titration of a solution 0.01 M of uranyl nitrate ($UO_2(NO_3)_2 \cdot 6H_2O$, purchased from Merck) with 0.05 M NaOH (Titrisol® grade, Merck). The system was thoroughly stirred, until a quantitative precipitation of metaschoepite in the pH range 4–5 occurred. The solid phase was separated from the mother liquor and stored in Milli-Q water at room temperature.

$Na_2U_2O_7 \cdot H_2O$(cr) was prepared by solid phase transformation of metaschoepite under alkaline pH conditions. A batch of metaschoepite was prepared as explained above in a solution with NaCl 1.0 M. The fresh precipitate was then quickly titrated with NaOH 0.1 M until pH = 11 was reached. A quantitative solid phase transformation was achieved in one week, marked by characteristic yellow-orange color of sodium uranate.

Before their use as starting materials for solubility experiments, the solid phases were equilibrated in aqueous solution at $T = 80$ °C for 30 days to ensure the same degree of crystallinity of the solid phases. To this purpose, metaschoepite was equilibrated in Milli-Q water, whereas sodium uranate was equilibrated in an aqueous solution containing 2.5 M NaCl and 0.05 M NaOH.

After equilibration, the U(VI) solids were isolated from the supernatant, washed, dried and characterized. X-ray diffraction (XRD) patterns of the dried powders were collected to gain information on the crystallinity degree of the different solids and the possible formation of alteration products. Measurements were performed on a Bruker AXS D8 Advance X-ray powder diffractometer at $5 \le 2\theta \le 60°$. Typically, incremental steps of 0.01°–0.04° were used and a measurement time: 4–30 s/step. The solid phases prepared were compared with the patterns of the reference crystalline metaschoepite (JSPD file n. 43-0364 [22]) and clarkeite (JCPDS file n. 50-1586 [23]). Quantitative chemical analyses were conducted on solutions of the dissolved solid phases (0.5–10 ppm U in 2% HNO_3) by means of inductively-coupled plasma-optical emission spectrometry (ICP-OES, Perkin – Elmer OPTIMA 2000™). Thermogravimetric analyses (TGA, Netsch STA 449 C) were used to study the thermal decomposition of the initial materials, in order to determine the relative stoichiometry of the crystallization water. Scanning electron spectroscopy with energy dispersive X-ray detector (SEM-EDS) was used to characterize the morphology and the particle size of the crystallites and to gain a qualitative elementary analysis to be compared with the results from ICP-OES. SEM pictures of the samples were taken with a CamScan CS 44 FE (Cambridge Instruments). Additional time-resolved laser-induced fluorescence (TRLFS) measurements were done to get a more complete analytical picture of the mentioned phases. Experiments were carried on a SpitLight Compact 100 (InnoLas Laser) instrument (methods are detailed in Section 2.3).

2.2 Solubility experiments

Solubility experiments from undersaturation conditions were performed in 0.10, 0.51 and 5.6 m NaCl solutions at $T = (25 \pm 1)$, (55 ± 1) and (80 ± 2) °C. Batch experiments (15–25 mL) were prepared in PTFE vials (Semadeni Plastic Group, Switzerland), according with the experimental setup described in Endrizzi et al. [15]. Solutions in the acidic pH_m-range were contacted with $UO_3 \cdot 2H_2O$(cr), while solutions in the alkaline pH_m range were contacted with $Na_2U_2O_7 \cdot H_2O$(cr). Solubility experiments were conducted in an Ar glovebox to exclude carbonate. Compact ovens/incubators (Falc Instruments) were placed into the glovebox for the batches equilibrating at 55 and 80 °C. Total concentration of uranium in solution and pH_m (with $pH_m = -\log [H^+]$, in molal units) were monitored for contact times of up to ~300 days (depending upon system/sample, see Table S2 in the supplementary information). pH_m was measured with a combination glass electrode (Orion ROSS). In samples with $[OH^-] > 0.03$ m, pH_m was instead calculated using K'_w for the corresponding ionic strength and temperature. Prior to the sampling, the electrode was calibrated against diluted commercial pH buffer solutions (Merck) at the same temperature of the samples, according to the procedure previously described [15]. The temperature dependence of the pH of the different buffer solutions

(from 0 °C to 90 °C) was provided by the manufacturer. pH_m values in the samples were determined from the experimentally measured pH_{exp} according with $pH_m = pH_{exp} + A_m$, where A_m is an empirical parameter entailing the activity coefficient of H^+ and the liquid junction potential of the electrode. Values of A_m in 0.10–5.6 m NaCl solutions at $T = 25$, 55, 80 °C were experimentally determined in this work as described previously [15]. The following empirical relation was derived from the experimental A_m values:

$$A_m = (2.779 \pm 0.002) - (1.649 \pm 0.002) \cdot 10^{-2} T + (0.288 \pm 0.002) m - (3.9 \pm 0.3) \cdot 10^{-4} Tm + (2.31 \pm 0.05) \cdot 10^{-5} T^2 + (5 \pm 11) \cdot 10^{-4} m^2$$

where T is the temperature in Kelvin and m is the molal concentration of the NaCl medium. Experimentally-determined values of A_m are listed in Table S1 as supplementary information. A numerical analysis of the parameters A_m with this empirical expression is shown in Figure S4 as supplementary information. Short-range extrapolation of A_m values outside such range of temperature and concentrations are possible (within ±10 K and ±0.1 m, Figure S4), however extrapolations to further ranges are not recommended.

During the sampling, vials were housed in a dry-block heater (*Ika*) and thermostated at the same temperature as during equilibration. Total uranium concentration was determined by ICP-MS after phase separation and corresponding dilution with 2% HNO_3. Phase separation was achieved by ultrafiltration (10 kD filters–NanoSep Merck Millipore) for samples equilibrated at $T = 25$ °C and rapid syringe filtration (Pall Acrodisc® filters, pore size 0.1 µm, PTFE membrane) for samples equilibrated at $T = 55$ and 80 °C. Values of concentration obtained in molar (M) units were converted to molal (m) units using the conversion factors reported in the TDB-NEA reviews for different background electrolytes [4].

2.3 Time-resolved laser-induced fluorescence spectroscopy

Time-resolved laser-induced fluorescence spectroscopy (TRLFS) measurements were performed using the 4th harmonic of a Nd:Yag laser at 266 nm and 7 ns pulse duration as excitation source. Data were collected at an energy of 0.6 mJ/pulse and 10 Hz repetition rate. Simultaneous control of the laser stability was possible by placing a beam splitter in the optic path and sending part of the beam to a thermopile sensor (Newport Corporation). Samples were prepared in small copper holders with sapphire windows and then introduced into the customized vacuum chamber of a He cryostat (CryVac) where temperatures as low as (6 ± 1) K are reached. Luminescence bands of most U(VI) solid phases or aqueous species appear normally in the blue-green part of the spectrum; however, in many cases those bands are clearly resolved only at very low temperatures [24, 25]. In the case of oxyhydroxide minerals, e. g. schoepite, broadening of the emission peaks due to quenching by OH-groups and water molecules can be reduced at low temperature, improving in this way the spectral resolution and increasing the spectral intensity. These improvements are also due to the reduction in the emission from thermally populated vibrational levels in the excited electronic state and the decrease of energy loss due to the suppressed vibrations [24]. The sample holder with capacity for two samples was directly attached to the cold finger of the cryostat. Once the laser beam reached the sample, the emitted light was collected at 90° by a customized bundle-type optic fiber. The output of the optic fiber was coupled to the variable entrance slit of a 0.3 focal length Czerny-Turner spectrometer (Shamrock SR 303i, Andor Technology) with a triple grating turret (400, 1200 and 2400 L/mm gratings), where the dispersed light was detected by a time-gated intensified CCD camera (iStar 734, Andor Technology). An external digital delay pulse generator (DG 535, Stanford Research Systems) was used to synchronize the data acquisition by the CCD camera with the sync output signal of the laser system. During the experiments, a long-pass filter (10CGA-295, Newport Corporation) was inserted into the spectrometer to avoid the second-order diffraction of the laser stray light at 532 nm.

2.4 Solution-drop calorimetry

Solution-drop calorimetry was used to study the acidic dissolution of $Na_2U_2O_7 \cdot H_2O$(cr) (2). Calorimetric experiments were conducted using 1.05 m $HClO_4$ as dissolution medium at $T = 25$, 45 and 80 °C. The enthalpy of reaction at $T = 55$ °C was then interpolated from the analysis of these data.

$$Na_2U_2O_7 \cdot H_2O(cr) + 6H^+ \rightarrow 2Na^+ + 2UO_2^{2+} + 4H_2O(l) \quad (2)$$

Microcalorimetric experiments were carried out at Lawrence Berkeley National Laboratory using a TAM Precision Solution Calorimeter (TA Instruments). The instrument offers high resolution of temperature due to the high-quality TAM III thermostat and modern electronics. The accuracy of the thermostatic bath is ±0.01–0.1 K around the real temperature value, depending on the exercise temperature, with better accuracy at lower temperatures.

The precision of the temperature around the temperature value declared by instrument is within ±10 µK. Short-time temperature fluctuations are smoothed by the presence of multiple electronically-controlled Peltier elements. With electronic noise reduction, the temperature resolution (precision) is close to 1 µK. Experimental control, data acquisition, graphical data presentation, data analysis, and result reports are computerized for the Precision Solution Calorimeter with the program Solcal (TA Instruments).

The calorimeter consists of a thin-walled 25 mL Pyrex-glass reaction vessel fitted with a thermistor for temperature sensing and a heater for calibration and equilibration. A weighed quantity of $Na_2U_2O_7 \cdot H_2O$(cr) (10–20 mg per experiment) was contained and sealed with epoxy resin in a specially designed glass ampoule (TA Instruments) that was mounted on the combined stirrer and ampoule holder. The combined stirrer and ampoule holder with the sample was inserted into the glass vessel containing 25 mL of 1.05 m $HClO_4$. As the desired thermal equilibrium was nearly achieved, the dissolution reaction was initiated by breaking the ampoule containing the sample and observed as an instantaneous change in temperature. Before and after the dissolution reaction took place, the system was calibrated electrically (i. e. a known amount of energy was added to the system to duplicate the effect of the thermal energy accompanying the dissolution processes). The small heat exchange with the environment during the reaction, the heat arising from stirring and the non-ideal thermal equilibrium conditions before and after the dissolution experiments were adjusted mathematically, using the information obtained from the baseline temperature changes before and after the experimental reaction. Duplicate or triplicate experiments were conducted at each temperature. An example of the instrument output diagram (offset temperature, mK vs. time, min) for a typical dissolution experiment of $Na_2U_2O_7 \cdot H_2O$(cr) is shown in Figure S5 as supplementary information.

The accuracy of the instrument was verified by conducting a dissolution experiment with KCl(cr) in water at 25 °C. The measured enthalpy of dissolution of KCl(cr) at 25 °C was 17.15 kJ/mol, in excellent agreement with the value (17.22 kJ/mol) in the literature [26].

3 Results

3.1 Solubility of $UO_3 \cdot 2H_2O$(cr) and $Na_2U_2O_7 \cdot H_2O$(cr)

Solubility data of metaschoepite and sodium uranate are shown in Figure 1 as the total concentration of dissolved uranium ([U(VI)], in molal units) vs. pH_m at $T = 25$, 55 and 80 °C. Figure 1 shows also solubility data obtained in previous studies conducted in 0.51 m NaCl at $T = 22$, 80 °C [15] and in 0.51–5.6 m NaCl at $T = 22$ °C [5].

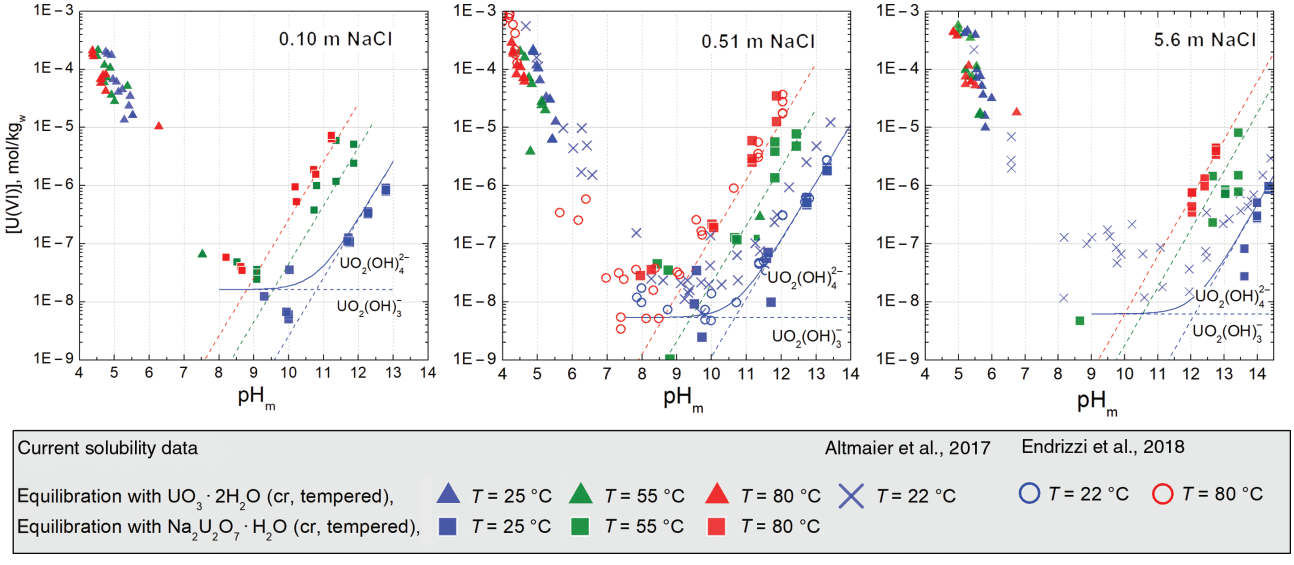

Figure 1: Solubility of $UO_3 \cdot 2H_2O$(cr) and $Na_2U_2O_7 \cdot H_2O$(cr) in 0.10, 0.51 and 5.6 m NaCl solutions at $T = 25$, 55 and 80 °C. Experimental data: U(VI) concentration vs. pH_m (–log [H^+]). Solid thick lines: SIT model calculations at $T = 25$ °C. Dashed lines: contribution to the solubility of the $UO_2(OH)_3^-$ (1,3) and $UO_2(OH)_4^{2-}$ (1,4) species. Solubility data reported in Altmaier et al. [5] and Endrizzi et al. [15] are also displayed for comparison.

The solubility of $UO_3 \cdot 2H_2O$(cr) at room temperature in acidic 0.51 m NaCl solutions compares well with solubility data determined by Altmaier et al. under the same conditions [5]. The solubility of the same material measured at $T = 55$ and 80 °C is lower (up to 1.0 order of magnitude at 80 °C) with respect to the corresponding one measured at room temperature at the same pH_m. Since the starting U(VI) solid material used in the solubility experiments at $T = 25$, 55 and 80 °C had been already equilibrated at 80 °C, we can basically exclude that this effect is related to an additional significant increase of solid phase crystallinity. In the acidic range, the concentration of U(VI) in solution is controlled by hydrolysis equilibria consuming ~2 H^+. Consistently, and in agreement with our previous findings, log [U(VI)] decreases linearly with pH_m following a well-defined slope of ~− 2.

In the near-neutral to moderately alkaline pH_m range, the solubility of uranium in 0.10 and 0.51 m NaCl solutions is ~10^{-8} m, also showing significant scattering of data. The concentration of U in these conditions is mostly independent of pH_m, indicating that no H^+ are involved in the solution equilibria controlling the solubility of U(VI) in this pH_m-region. A relatively high uncertainty is associated to measured solubilities in this pH_m range. Accordingly, a defined effect of the temperature on the solubility of uranium in the near-neutral to moderately alkaline pH_m-range could not be confirmed within this work.

In the alkaline and hyper-alkaline pH range, the solubility of sodium uranate increases with pH_m with a well-defined slope of +1 (log [U(VI)] vs. pH_m), indicating the release of one H^+ in the equilibrium reaction controlling the solubility of U(VI). At $T = 25$ °C, the solubility of $Na_2U_2O_7 \cdot H_2O$(cr) in 0.51 m NaCl is very similar to previous solubility results using a $Na_2U_2O_7 \cdot H_2O$(cr) phase previously equilibrated at 80 °C [15]. In addition, and consistently with data reported in Endrizzi et al., the solubility was found to be systematically lower (~0.3 $\log_{10}$-units) than the one determined by Altmaier et al. with a batch of $Na_2U_2O_7 \cdot H_2O$(cr) prepared and used at room temperature [5]. The observed small decrease in the solubility of sodium uranate is likely related to an increase of crystallinity of the initial material as an effect of temperature. A very good reproducibility was observed between the solubility of $Na_2U_2O_7 \cdot H_2O$(cr) at $T = 80$ °C in the present work and the one previously reported [15]. In the alkaline and hyper-alkaline pH region, the solubility of sodium uranate is significantly enhanced by temperature: the concentrations of uranium in the contacting solutions at $T = 55$ and 80 °C are higher than the corresponding ones at room temperature by means of 1.3–1.7 and 2.1–2.5 orders of magnitude, respectively (Figure 1).

3.2 Solid phase characterization

3.2.1 Metaschoepite

Figure 2 shows the XRD patterns of (a) the reference compounds $UO_3 \cdot 2H_2O$(cr) (JSPD file 43-0364 [22]), $Na(UO_2)O(OH)$(cr) ("clarkeite", JSPD file 50-1586 [23]) and $Na_2U_3O_{10} \cdot H_2O$(cr) (JSPD file 41-0840 [27]), (b) the $UO_3 \cdot 2H_2O$(cr) "starting material" prepared as described in Section 2.1, and $UO_3 \cdot 2H_2O$(cr) after completing the solubility experiments in (c) 0.10 m NaCl, $T = 25$ °C, $pH_m = 4.8$; (d) 0.10 m NaCl, $T = 80$ °C, $pH_m = 4.4$; (e), 0.51 m NaCl, $T = 25$ °C, $pH_m = 4.9$; (f), 0.51 m NaCl, $T = 80$ °C, $pH_m = 4.5$; (g) 5.6 m NaCl, $T = 25$ °C, $pH_m = 5.6$; (h) 5.6 m NaCl, $T = 80$ °C, $pH_m = 4.9$. The values of the Na:U molar ratio quantified by elementary analyses (ICP-OES and SEM-EDS) are also reported in the figure.

The diffractogram of $UO_3 \cdot 2H_2O$(cr) "starting material" in Figure 2b shows the characteristic pattern of metaschoepite (Figure 2a, red, JSPD File n. 43-0364 [22]), with main peaks at $2\theta = 12.1$, 24.2, 24.8, 25.5 deg. TGA diagrams of $UO_3 \cdot 2H_2O$(cr) are shown in Figures S1 and S2 in the supplementary information. $UO_3 \cdot 2H_2O$(cr) decomposed with a percentage weight loss of 10.9–12.2 % in the temperature range 100–675 °C, consistent with the loss of two water molecules. Elementary analyses conducted with ICP-OES and with SEM-EDS excluded the presence of Na in the obtained solid materials. SEM analysis revealed the expected platelet-like structure of the crystallites, featuring an average diameter in the range 0.5–3 μm (Figure S3 in the supplementary information).

Characterization of solid phases of $UO_3 \cdot 2H_2O$(cr) isolated after the solubility experiments indicate that the "starting material" $UO_3 \cdot 2H_2O$(cr) remained stable in all NaCl solutions equilibrated at $T = 25$ °C. XRD spectra did not show feature patterns assigned to sodium-uranate-like phases (Figure 2c, e, g). Furthermore, quantitative chemical analysis of the solid phase conducted by ICP-OES supported the absence of Na in the solid phase.

The batch of $UO_3 \cdot 2H_2O$(cr) equilibrated in a 0.10 m NaCl solution at $T = 80$ °C shows a minor inclusion of Na (Na:U = 0.07). The XRD diffractogram of this solid phase (Figure 2d) does not show features consistent with sodium uranate ("clarkeite", reference JSPD file n. 50-1586 [23] in Figure 2a, blue) or other known sodium uranate-like phases ($Na_2U_3O_{10} \cdot H_2O$, ref. JSPD file n. 41-0840 [27] in Figure 2a, green). A solid phase transformation of metaschoepite to a sodium uranate-like material is observed, instead, in batches of $UO_3 \cdot 2H_2O$(cr) contacted with acidic solutions ($pH_m \geq 4.4$) of 0.51 m NaCl at $T = 80$ °C. The XRD spectrum of the material collected from experiments in 0.51 m

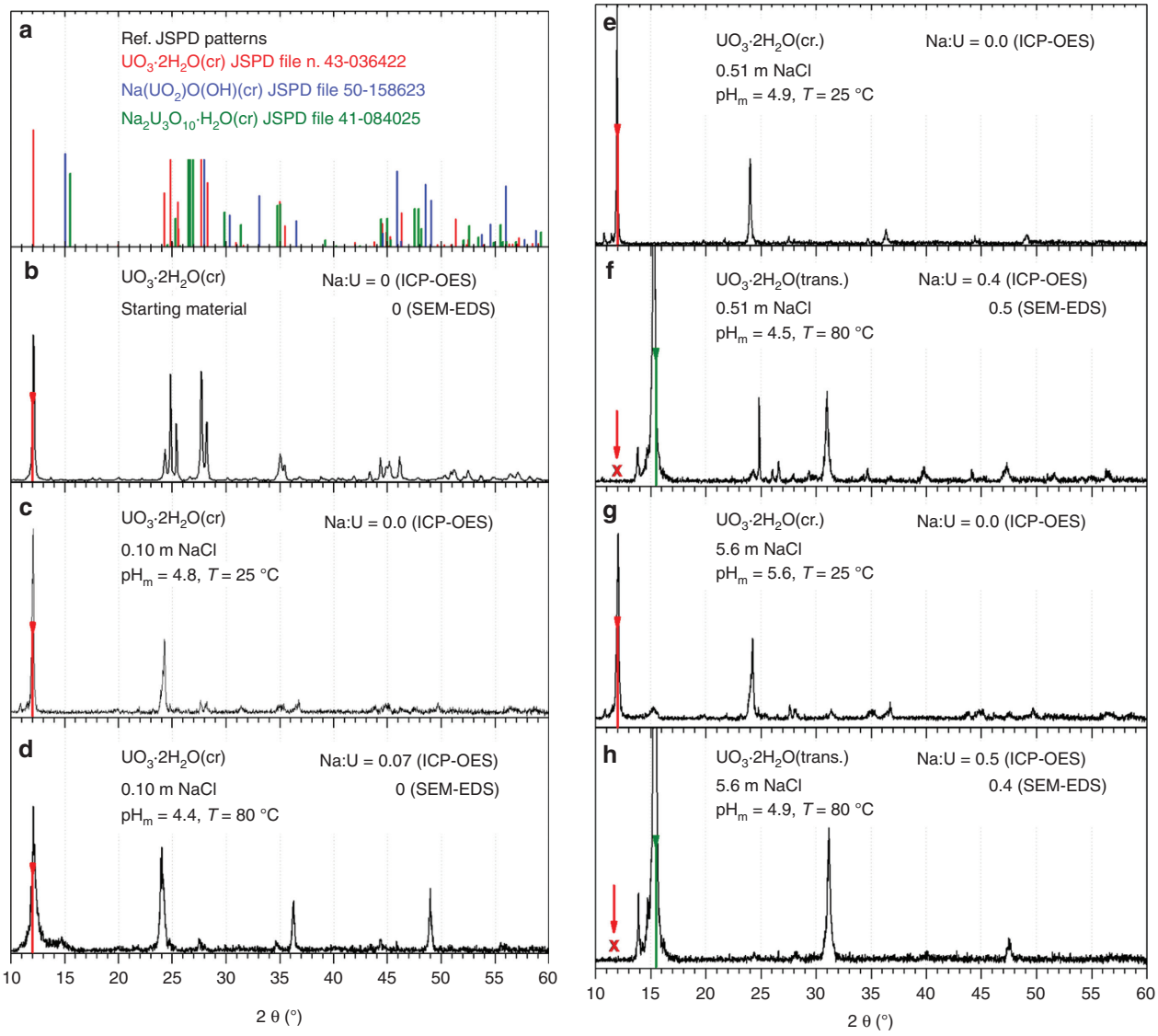

Figure 2: Powder XRD patterns of $UO_3 \cdot 2H_2O$(cr) investigated in the p.w.
(a) Reference patterns of $UO_3 \cdot 2H_2O$(cr) (red, JSPD file 43-0364 [22]), $Na(UO_2)O(OH)$(cr) (blue, JSPD file 50-1586 [23]), $Na_2U_3O_{10} \cdot H_2O$(cr) (green, JSPD file 41-0840 [27]). (b) $UO_3 \cdot 2H_2O$(cr) before solubility experiments, "starting material" (pre-equilibrated in water at $T = 80$ °C). (c) $UO_3 \cdot 2H_2O$(cr) equilibrated 260 days, $T = 25$ °C, 0.10 m NaCl, $pH_m = 4.8$. (d) $UO_3 \cdot 2H_2O$(cr) equilibrated 260 days, $T = 80$ °C, 0.10 m NaCl, $pH_m = 4.4$. (e) $UO_3 \cdot 2H_2O$(cr) equilibrated 260 days, $T = 25$ °C, 0.51 m NaCl, $pH_m = 4.5$. (f) $UO_3 \cdot 2H_2O$(trans.) equilibrated 260 days, $T = 80$ °C, 0.51 m NaCl, $pH_m = 4.9$. (g) $UO_3 \cdot 2H_2O$(cr) equilibrated 260 days, $T = 25$ °C, 5.6 m NaCl, $pH_m = 5.6$. (h) $UO_3 \cdot 2H_2O$(trans.) equilibrated 260 days, $T = 80$ °C, 5.6 m NaCl, $pH_m = 4.9$.

NaCl at $T = 80$ °C (Figure 2f) shows two distinct peaks at $2\theta = 15.3$, 31.0 deg. that could be assigned to a sodium-uranate-like phase, although not matching exactly with the peaks of the reference sodium uranate ($2\theta = 15.0$, 30.3, 33.0 deg., Figure 2a, blue). The peak at $2\theta = 12.1$, assigned to metaschoepite, is instead clearly absent. Similar observations were obtained in Endrizzi et al. with metaschoepite equilibrated in 0.51 m NaCl at $T = 80$ °C [15]. ICP-OES and EDX elementary analyses indicate a molar ratio Na:U = 0.4–0.5, also in very good agreement with previous findings [15]. The current new results indicate that a solid phase transformation of metaschoepite occurs under these conditions, leading to a non-stoichiometric solid phase $Na_{0.4}UO_{3.2} \cdot 1.4H_2O$(s) or similar.

The batch of metaschoepite equilibrated in 5.6 m NaCl at $T = 80$ °C (Figure 2h) shows XRD patterns very similar to those of the solid equilibrated in 0.51 m NaCl (Figure 2f), and the same Na:U molar ratio (0.4–0.5). This result suggests that the same alteration product was possibly obtained at the end of the experiments in 0.51 and

5.6 m NaCl solutions, hinting that the transformation of metaschoepite at the end of the solubility experiments at $T = 80\,°C$ in these two media is complete, and hence the transformed phase stable under these equilibration conditions.

Figure 3 shows the TRLFS emission spectra at near liquid He temperature (6 K) of the initial metaschoepite (sample is corresponding to the XRD pattern in Figure 2b) and transformed metaschoepite (equilibrated in 0.51 m NaCl at $T = 80\,°C$, $pH_m = 4.5$, corresponding to the XRD pattern in Figure 2f). As discussed in Section 2.3, depending on the ligand system, uranyl luminescence emission at room temperature can be very weak, e. g. for pure uranyl carbonate complexes, but easier to detect at liquid He temperature. A first attempt to collect the emission spectra at room temperature failed, and data are not shown in the figure. In Figure 3 the acquisition was performed with a 400 lines/mm diffraction grating. Spectral feature typical from uranyl compounds can be observed in both spectra including vibronic bands with specific peak spacing, or peak maxima. In both cases the position of the spectral bands are red-shifted as compared to those from carbonates or phosphate uranyl minerals [28, 29]. The mentioned spacing between the vibronic bands corresponds to the symmetric stretching frequency of the O=U=O moiety [24]. This frequency is inversely correlated to the strength of the coordination of U(VI) with the coordination ligand in the equatorial plane. The ν_1 values measured in both solid phases are between 720 and 780 cm^{-1}. Usually low symmetric stretching frequency values are associated to minerals of uranyl silicate and oxyhydroxide. This fact can be explained by the stronger ionic interaction of uranyl (hard acid) with anions with stronger basicity (larger pK_a values) [29]. A bathochromic shift of ~5 nm in the position of the first-peak maxima is also observed for the transformed metaschoepite. According to Gorobetts et al. [30] an increase of the basicity of the molecules in the uranyl solvation or coordination sphere could induce a shift of the luminescence spectrum to low frequencies. The reason is a stronger chemical bond of the uranium atom with the ligand and a weakening of the stretching in the U=O bond.

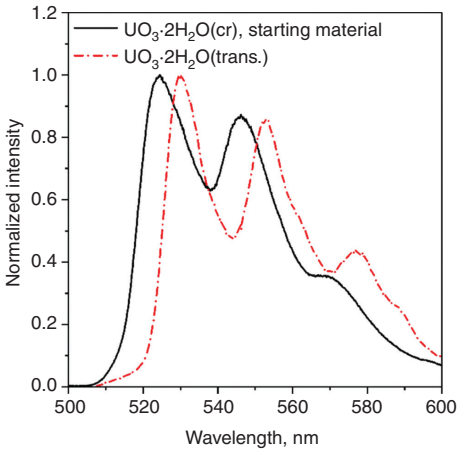

Figure 3: Luminescence spectra of metaschoepite "starting material" (solid line) and transformed metaschoepite (equilibrated in 0.51 m NaCl at $T = 80\,°C$, $pH_m = 4.5$ short dash dot line). Spectra measured at ~6 K, 1 µs delay, 1 ms integration time, 500 accumulations. Laser: $\lambda_{ex} = 266$ nm; 600 µJ/pulse.

Luminescence lifetimes were also calculated for the metaschoepite "starting material" and transformed metaschoepite, obtaining in both cases a bi-exponential decay. In the case of metaschoepite "starting material", the two components of the decay are: (15.4 ± 0.3) µs and (81.8 ± 0.6) µs. For the transformed metaschoepite both lifetimes are shorter, namely (5.6 ± 0.8) µs and (63.2 ± 35.2) µs. This effect has been already observed for uranyl minerals at low temperature [28, 29, 31, 32]. Volodko et al. [31] explained the bi-exponential decay as a redistribution of energy occurring after excitation. Instead, Perry and Brittain [32] proposed the presence of two geometrically similar uranyl coordination environments.

3.2.2 Sodium uranate

Figure 4 shows the XRD patterns of (a) the reference compounds $Na(UO_2)O(OH)$(cr) ("clarkeite", JSPD file 50-1586 [23]) and $Na_2U_3O_{10} \cdot H_2O$(cr) (JSPD file 41-0840 [27]), (b) the sodium uranate "starting material" prepared as described in Section 2.1, and selected sodium uranate samples collected after completing the solubility experiments at $T = 80\,°C$ in (c) 0.10 m NaCl, $pH_m = 8.4$; (d) 0.51 m NaCl, $pH_m = 12.0$, (e) 0.51 m NaCl, $pH_m = 8.3$ and (f) 0.51 m NaCl, $pH_m = 11.2$. The values of the Na:U molar ratio quantified by elementary analyses (ICP-OES and SEM-EDS) are also reported in the figure.

The diffraction pattern of the sodium uranate "starting material" is consistent with the reference clarkeite (Figure 4a JSPD file 50-1586 [23]), with relevant peaks at $2\theta = 15.0$, 26.4, 27.6, 30.4 deg. Elemental analyses by ICP-OES further confirms a molar ratio Na:U = 1 in this solid phase. Figure S2 as supplementary information shows the TGA diagram of the same "starting material". The solid decomposed with a weight loss of 2.5–2.6 % in the temperature range 50–550 °C, consistent with the loss of 0.9 water molecules. However, a clear plateau was not reached at the end of the experiments, suggesting that the decomposition of sodium uranate with release of water was not a quantitative process, consistently with the

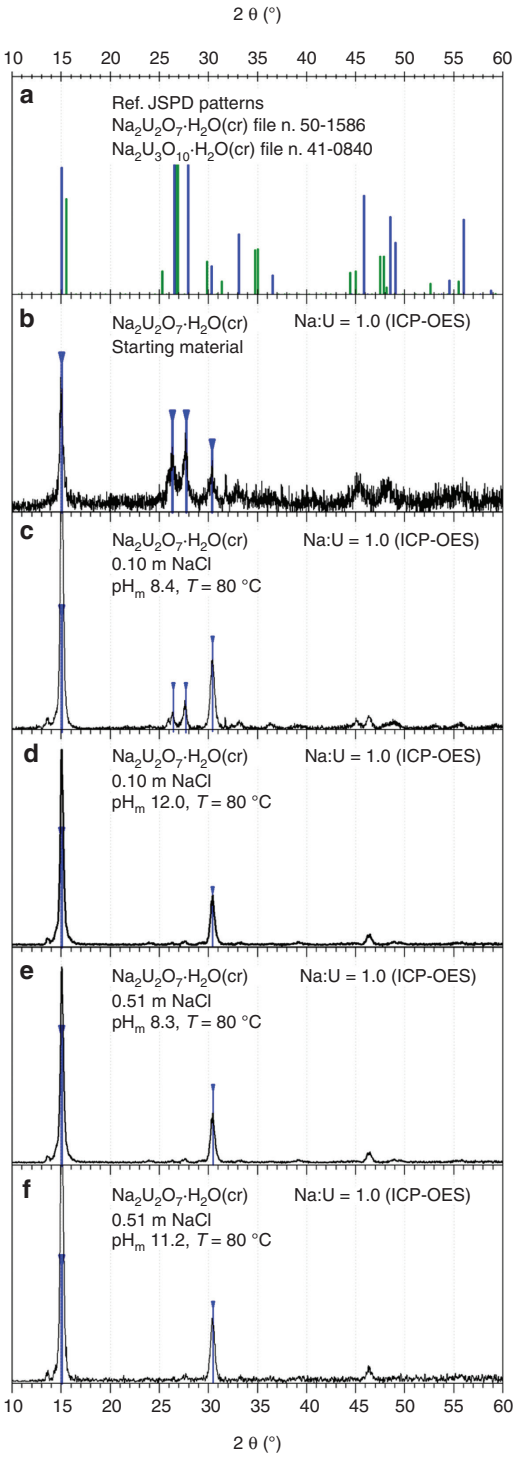

Figure 4: Powder XRD patterns of $Na_2U_2O_7 \cdot H_2O$(cr) investigated in the p.w.
(a) Blue: reference patterns of $Na(UO_2)O(OH)$(cr) (JSPD file 50-1586 [23]); green: reference patterns of $Na_2U_3O_{10} \cdot H_2O$(cr) (JSPD file 41-0840 [27]). (b) $Na_2U_2O_7 \cdot H_2O$(cr) before solubility experiments. Pre-equilibrated at $T = 80$ °C. (c) $Na_2U_2O_7 \cdot H_2O$(cr) equilibrated 292 days, $T = 80$ °C, NaCl 0.10 m, $pH_m = 8.4$. (d) $Na_2U_2O_7 \cdot H_2O$(cr) equilibrated 292 days, $T = 80$ °C, NaCl 0.10 m, $pH_m = 12.0$. (e) $Na_2U_2O_7 \cdot H_2O$(cr) equilibrated 268 days, $T = 80$ °C, NaCl 0.10 m, $pH_m = 8.3$. (f) $Na_2U_2O_7 \cdot H_2O$(cr) equilibrated 292 days, $T = 80$ °C, NaCl 0.51 m, $pH_m = 11.2$.

observations in a previous study [33]. Elementary analyses by ICP-OES and SEM-EDS indicated a 1:1 Na:U molar ratio and the absence of chloride in the solid. All these observations confirm that the "starting material" can be assigned as $Na_2U_2O_7 \cdot H_2O$(cr).

XRD and elementary analyses of the solid phases collected at the end of the solubility experiments in alkaline conditions at $T = 80$ °C further confirm that the "starting material" was not altered in the course of the solubility experiments and thus that $Na_2U_2O_7 \cdot H_2O$(cr) is thermodynamically stable in all the experimental conditions investigated (Figure 4d–f).

3.3 Solubility and hydrolysis model of $UO_3 \cdot 2H_2O$(cr) and $Na_2U_2O_7 \cdot H_2O$(cr)

3.3.1 Solubility and hydrolysis model at $T = 25$ °C

To determine $\log {}^*K^\circ_{s,0}\{UO_3 \cdot 2H_2O(cr)\}$, data collected from solubility experiments at $T = 25$ °C were analyzed together with a least-square minimization procedure. The speciation model included the values of the U(VI) hydrolysis constants in the acidic range recommended by the NEA-TDB [4] and adopted by Altmaier et al. and Endrizzi et al. [5, 15]. The SIT model and the related SIT parameters reported by Altmaier et al. [5] were used to apply the necessary corrections to account for the effect of the ionic medium.

The available hydrolysis model of U(VI) in the pH_m range 4.0–5.5 at room temperature [4, 5] (Table 1) predicts that the species UO_2^{2+} and $(UO_2)_2(OH)_2^{2+}$ dominate the aqueous speciation of U(VI) under these conditions. In agreement with previous results by Endrizzi et al. [15], this is consistent with the linear trend of log [U(VI)] vs. pH_m with a slope of –2, as observed from the solubility data collected at room temperature in this pH_m range.

The value of the solubility constant of $UO_3 \cdot 2H_2O$(cr), $\log {}^*K^\circ_{s,0} = (5.1 \pm 0.2)$ ($T = 25$ °C, $I = 0$, Table 1) was determined from the solubility data (log [U(VI)] vs. pH_m) in 0.10, 0.51 and 5.6 m NaCl solutions. This value is in good agreement with $\log {}^*K^\circ_{s,0} = (5.35 \pm 0.13)$ determined in our previous study with a solid phase pre-equilibrated only at $T = 22$ °C (instead of $T = 80$ °C in Milli-Q water as in the present work) [5]. This observation reflects that a tempering step at $T = 80$ °C (in the absence of NaCl as background electrolyte) has a relatively minor impact on the crystallinity of the initial $UO_3 \cdot 2H_2O$(cr) solid phase.

A thermodynamic model describing the solubility and hydrolysis of $Na_2U_2O_7 \cdot H_2O$(cr) in the moderately to hyperalkaline pH_m region was also derived. In the moderately alkaline region, $Na_2U_2O_7 \cdot H_2O$(cr) exhibits a low solubility

Table 1: Thermodynamic data derived in the present work or reported in the literature for selected reactions.

Solid phases	Notes	$\log {}^{*}K_s^\circ \pm 2\sigma$	$\Delta^{*}H_s \pm 2\sigma$ kJ/mol	T, °C	Ref.
$UO_3 \cdot 2H_2O(cr) + 2H^+ = UO_2^{2+} + 3H_2O(l)$	[a]	**(5.1 ± 0.2)**		**25**	**p.w.**
	[b]	(5.35 ± 0.13)		22	
$0.5Na_2U_2O_7 \cdot H_2O(cr) + 3H^+ = Na^+ + UO_2^{2+} + 2H_2O(l)$	[a,c]	**(11.7 ± 0.2)**	**–(66.4 ± 0.4)**	**25**	**p.w.**
	[a,d]		**–(67.9 ± 0.4)**	**25**	**p.w.**
	[a,c]		**–(63.6 ± 0.3)**	**45**	**p.w.**
	[a,d]		**–(64.9 ± 0.3)**	**45**	**p.w.**
	[a,c]	**(10.7 ± 0.2)**	**–(62.9 ± 0.3)**	**55**	**p.w.**
	[a,c]	**(10.0 ± 0.3)**	**–(60.8 ± 0.2)**	**80**	**p.w.**
	[a,d]		**–(61.7 ± 0.2)**	**80**	**p.w.**
	[a]	(11.9 ± 0.4)		22	[15]
	[b]	(12.2 ± 0.2)		22	[5]
$0.5Na_2U_2O_7 \cdot H_2O(cr) + 2H_2O(l) = Na^+ + UO_2(OH)_4^{2-} + H^+$	[a,c]	**–(20.2 ± 0.3)**		**25**	**p.w.**
	[a,c]	**–(19.0 ± 0.5)**	**(71 ± 3)**	**55**	**p.w.**
	[a,c]	**–(18.3 ± 0.4)**		**80**	**p.w.**
	[a]	–(20.1 ± 0.3)	(72 ± 4)	22	[15]
	[a]	–(18.0 ± 0.1)		80	[15]
	[b]	–(19.7 ± 0.3)		22	[5]
Hydrolysis species	**Notes**	$\log {}^{*}\beta^\circ \pm 2\sigma$	$\Delta^{*}H^\circ \pm 2\sigma$, kJ/mol		
$UO_2^{2+} + H_2O(l) = UO_2(OH)^+ + H^+$		–(5.25 ± 0.24)		25	[4]
$UO_2^{2+} + 2H_2O(l) = UO_2(OH)_2(aq) + 2H^+$		–(12.15 ± 0.17)		25	[4]
$2UO_2^{2+} + 2H_2O(l) = (UO_2)_2(OH)_2^{2+} + 2H^+$		–(5.62 ± 0.04)		25	[4]
$3UO_2^{2+} + 4H_2O(l) = (UO_2)_3(OH)_4^{2+} + 4H^+$		–(11.9 ± 0.3)		25	[4]
$3UO_2^{2+} + 5H_2O(l) = (UO_2)_3(OH)_5^{+} + 5H^+$		–(15.55 ± 0.12)		25	[4]
$3UO_2^{2+} + 7H_2O(l) = (UO_2)_3(OH)_7^{-} + 7H^+$		–(32.2 ± 0.8)		25	[4]
$4UO_2^{2+} + 7H_2O(l) = (UO_2)_4(OH)_7^{+} + 7H^+$		–(21.9 ± 1.0)		25	[4]
$UO_2^{2+} + 3H_2O(l) = UO_2(OH)_3^{-} + 3H^+$		–(20.7 ± 0.4)		25	[5]
$UO_2^{2+} + 4H_2O(l) = UO_2(OH)_4^{2-} + 4H^+$		**–(31.9 ± 0.2)**		**25**	[5]
	[e]	**–(29.7 ± 0.4)**	**(134 ± 14)**	**55**	**p.w.**
		–(28.0 ± 0.3)		**80**	**p.w.**
Water autoprotolysis		**$\log K_w^\circ$**	**$\Delta_r H^\circ$, kJ/mol**		
$H_2O(l) = H^+ + OH^-$		**–14.00**	**55.83**	**25**	[34]
		–13.15	**50.23**	**55**	[34]
		–12.61	**45.57**	**80**	[34]

Values in bold face are selected in the present work for modelling thermodynamic data or derived in the present work from the current experimental data (p.w.).

[a]Solid phase pre-equilibrated at $T = 80$ °C. [b]Solid phase prepared at $T = 25$ °C and not pre-equilibrated at higher temperatures. [c]Enthalpy value determined from solution-drop microcalorimetric data and corrected to $I = 0$ with calculation by means of SIT. [d]Enthalpy value determined from solution-drop microcalorimetric data in 1.05 m $HClO_4$. [e]Enthalpy value determined from solution-drop microcalorimetric data and solubility data at dfferent temperatures; value corrected to $I = 0$ with calculation by means of SIT.

($10^{-8} - 10^{-9.2}$ m), which is controlled by the formation of $UO_2(OH)_3^-$ [(1) with $x = 3$] and consistent with a pH_m-independent process. In the alkaline and hyper-alkaline pH_m regions (up to $pH_m = 14.3$ in 5.6 m NaCl) the solubility of $Na_2U_2O_7 \cdot H_2O(cr)$ is controlled by the formation of $UO_2(OH)_4^{2-}$ [(1) with $x = 4$], as observed by the increase of solubility with a slope of +1 in the trend of log [U(VI)] vs. pH_m (Figure 1).

The solubility product of $Na_2U_2O_7 \cdot H_2O(cr)$, was determined by numerical minimization of the solubility data (log [U(VI)] vs. pH_m) at $T = 25$ °C, assuming a speciation model consistent with the formation of the two monomeric

species $UO_2(OH)_3^-$ and $UO_2(OH)_4^{2-}$. The hydrolysis constants of the two complexes, together with the related SIT parameters, were selected from recently published data by Altmaier et al. [5], also being consistent with the approach adopted in the publication of Endrizzi et al. [15] The quality of the result of the numerical analysis is reasonably good ($\sigma = 0.39$) considering the relative sparsity of the data.

$$0.5Na_2U_2O_7 \cdot H_2O(cr) + 3H^+ = Na^+ + UO_2^{2+} + 2H_2O(l) \quad (3)$$

$$\log {}^*K^\circ_{s,0} = (11.7 \pm 0.2)\ (T = 25\ ^\circ C,\ I = 0)$$

Blue solid lines in Figure 1 show the solubility of $Na_2U_2O_7 \cdot H_2O(cr)$ calculated at $T = 25\ ^\circ C$ using $\log {}^*K^\circ_{s,0}$ derived in this work as well as $\log {}^*\beta^\circ_{1,x}$ and $\varepsilon(UO_2(OH)_x^{2-x}, Na^+)$ (with $x = 3$–4) reported in Altmaier et al. [5]. Blue dashed lines in the figure represent the individual contributions of the species $UO_2(OH)_3^-$ and $UO_2(OH)_4^{2-}$. The calculated value of $\log {}^*K^\circ_{s,0}$ is in good agreement with $\log {}^*K^\circ_{s,0} = (11.9 \pm 0.4)$ determined in Endrizzi et al. for a $Na_2U_2O_7 \cdot H_2O(cr)$ solid phase also tempered at $T = 80\ ^\circ C$ [15]. This is consistent with the excellent agreement of the solubility data in 0.51 m NaCl solutions determined in both studies (Figure 1).

3.3.2 Enthalpy of dissolution of $Na_2U_2O_7 \cdot H_2O(cr)$

The heats developed by the dissolution of $Na_2U_2O_7 \cdot H_2O(cr)$ in 1.05 m $HClO_4$, measured by means of solution-drop calorimetry were $-(135.813 \pm 0.516)$, $-(129.884 \pm 0.232)$, $-(123.312 \pm 0.080)$ kJ/mol at $T = 25$, 45, 80 °C, respectively (Table 1). We quantitatively attribute the measured heats to the dissolution reaction enthalpy $\Delta^* H'_s$ (3) (Section 2.4).

Thermal contributions due to the dilution of Na^+ and UO_2^{2+} in 1.05 m $HClO_4$[1] are certainly small with respect to the reaction heat (within the assigned uncertainties of the measured heats themselves), and can be neglected [35, 36]. The value of $\Delta^* H'_s$ at 55 °C was determined by interpolation of the experimental data at 25, 45 and 80 °C (Table 1). The corresponding values of the heat of dissolution $\Delta^* H^\circ_s(T)$ at $I = 0$ are $-(133.2 \pm 1.1)$, $-(127.4 \pm 1.3)$, $-(121.5 \pm 1.5)$ at $T = 25$, 55 and 80 °C, respectively [Table 1, values listed are relative to the reaction involving 0.5 equivalents of $Na_2U_2O_7 \cdot H_2O(cr)$ (3)]. $\Delta^* H^\circ_s(T)$ at $I = 0$ were calculated as in (3) using (4) as described in Grenthe et al. [37].

$$\Delta^* H^\circ_s(T) = \Delta^* H'_s - 4L_1 - 2L_{2,Na^+} - 2L_{2,UO_2^{2+}} + 6L_{2,H^+} \quad (4)$$

In (4), L_1 is the relative partial molar enthalpy of water, L_2 are the relative partial molar enthalpies of dissolution of the individual aqueous species involved in (3). The values of the relative partial molar enthalpies of water and of the other species were estimated using the SIT model as described in (5) and (6) [37].

$$L_1 = M_w\left(-\frac{3}{2}\frac{A_L}{1.5^3}\left(t - 2\ln t - \frac{1}{t}\right) + RT^2 m_{HClO_4}\epsilon_L(H^+, ClO_4^-)\right) \quad (5)$$

$$L_{2,i} = \frac{3}{4}\frac{A_L Z_i^2 \sqrt{I_m}}{t} - RT^2 m_j \epsilon_L(i, j) \quad (6)$$

where M_w is the molar mass of water in kg/mol, $R = 8.314$ J K^{-1} mol^{-1}, $t = 1 + 1.5\sqrt{I}$ ($I = 1.05$ m $HClO_4$), A_L (kg mol$^{-1/2}$) is the Debye-Hückel parameter for the enthalpy in aqueous systems at the different temperatures, tabulated in Ref. [38]. $\epsilon_L(i, j) = (\partial\epsilon(i, j)/\partial T)_p$ is the temperature derivative of the SIT interaction parameters $\epsilon(i, j)$ of the pair of the ion i and the counter-ion of the ionic medium j. The required values of $\epsilon_L(i, j)$ were derived in the present work from the corresponding temperature derivatives of the Pitzer interaction parameters, available in Ref. [38]: $\epsilon_L(Na^+, ClO_4^-) = (3.72 \pm 0.05)\cdot 10^{-3}$ kg mol^{-1} K^{-1}, $\epsilon_L(H^+, ClO_4^-) =$ $(1.84 \pm 0.03)\cdot 10^{-3}$ kg mol^{-1} K^{-1}. In the literature, no temperature derivatives of the Pitzer interaction parameters of the (UO_2^{2+}, ClO_4^-) pair are available. A reasonable estimate of $\epsilon_L(UO_2^{2+}, ClO_4^-) \sim (5 \pm 1)\cdot 10^{-3}$ kg mol^{-1} K^{-1} was therefore given on the basis of the available parameters for different (M^{2+}, ClO_4^-) ion pairs [38]. As generally expected [39], the ionic medium has an almost negligible impact on the reaction enthalpy. The values of $\Delta^* H^\circ_s(T)$ and $\Delta^* H'_s(T)$ at $I = 1.05$ m $HClO_4$ are close to one another within ~1.5 kJ/mol (Table 1).

To the best of the authors' knowledge, no other determinations of the dissolution enthalpy of hydrated $Na_2U_2O_7 \cdot H_2O(cr)$ solid materials exist to date in the literature. The dissolution heat of anhydrous $Na_2U_2O_7(cr)$ solids has instead been reported in different calorimetric studies and summarized in the NEA-TDB critical reviews [4, 40]. The value of $\Delta^* H'_s$ ($Na_2U_2O_7(cr)$, 25 °C, 1 M HCl) $= -(171.8 \pm 1.0)$ kJ/mol selected in the NEA-TDB [4], together with the corresponding standard formation enthalpy (see next section), is the one determined calorimetrically by Tso

1 The dilution heat is the heat of transfer of Na^+, UO_2^{2+} in solution, from conditions of their infinite dilution, to *ca.* $1.8 \cdot 10^{-3}$ m, the maximum final concentration expected when dissolving 10–15 mg of solid phase in 25 mL of solution (see Section 2.3).

et al. [41]. In a similar calorimetric study, Cordfunke et al. [42] determined a value of Δ^*H_s' ($Na_2U_2O_7$(cr), 25 °C, 6 M HNO_3) = –(184.35 ± 1.13) kJ/mol. A rough estimation of the corresponding value of $\Delta^*H_s^\circ$ at $I = 0$ is provided in the present work, using the same method described above. This yields: Δ^*H_s ($Na_2U_2O_7$(cr), 25 °C, $I = 0$) = –(175 ± 5) kJ/mol. The comparison of $\Delta^*H_s^\circ$ of $Na_2U_2O_7 \cdot H_2O$(cr) in the present work with the one selected in the NEA-TDB for the anhydrous $Na_2U_2O_7$(cr) yields a net exothermal contribution of –(39 ± 1) kJ/mol for the formal hydration reaction of $Na_2U_2O_7$(cr) (7). A value comparable within the uncertainties is obtained from the comparison of the analogous data by Cordfunke et al. [42] at $I = 0$, –(42 ± 5) kJ/mol.

$$Na_2U_2O_7(cr) + H_2O(l) = Na_2U_2O_7 \cdot H_2O(cr) \quad (7)$$

3.3.3 Free-energy and enthalpy of formation of $Na_2U_2O_7 \cdot H_2O$(cr)

The values of the free-energy and enthalpy of formation of the $Na_2U_2O_7 \cdot H_2O$(cr) ($\Delta_f G_m^\circ$ and $\Delta_f H_m^\circ$) characterized in the present work are $\Delta_f G_m^\circ = -(3244 \pm 4)$ kJ/mol and $\Delta_f H_m^\circ = -(3531 \pm 16)$ kJ/mol (Table 2). $\Delta_f G_m^\circ$ was calculated from the solubility constant $\log {}^*K_{s,0}^\circ$ at $T = 25$ °C, whereas $\Delta_f H_m^\circ$ was calculated from the experimental value of $\Delta^*H_s^\circ$ at $T = 25$ °C. The values of $\Delta_f G_m^\circ$ and $\Delta_f H_m^\circ$ of the individual aqueous species reported in the NEA-TDB [4] were used in the calculations.

In a recent study by Smith et al. [43] using Knudsen-Effusion Mass-Spectrometry, a value of $\Delta_f H_m^\circ = -(3208.4 \pm 5.5)$ kJ/mol was determined for the α-$Na_2U_2O_7$(cr) (Table 2). The same authors reported also a two-parameter empirical equation to linearly relate $\Delta_f G_m^\circ$ of the solid phase with T, applicable in the high-temperature range from 1292 to 1481 K. The values of $\Delta_f G_m^\circ$ and $\Delta_f H_m^\circ$ ($T = 25$ °C) selected in the NEA-TDB [4] for the crystalline anhydrous $Na_2U_2O_7$(cr) (see Table 2) were taken from the calorimetric study by Tso et al. [41]. We note the good agreement in the values of $\Delta_f H_m^\circ$ determined by Smith et al. [43] and Tso et al. [41] using two different techniques.

Table 2: Free-energy and enthalpies of formation of $Na_2U_2O_7 \cdot H_2O$(cr) (present work) and comparison with literature values for anhydrous $Na_2U_2O_7$(cr) materials ($T = 298.15$ K).

Solid phase	$\Delta_f G_m^\circ \pm 2\sigma$, kJ/mol	$\Delta_f H_m^\circ \pm 2\sigma$, kJ/mol	Ref.
$Na_2U_2O_7 \cdot H_2O$(cr)	–(3244 ± 4)	–(3531 ± 16)	p.w.
$Na_2U_2O_7$(cr)	–(3011.5 ± 4.0)	–(3203.8 ± 4.0)	[4]
α-$Na_2U_2O_7$(cr)		–(3208.4 ± 11)	[43]

The difference between $\Delta_f G_m^\circ$ of the anhydrous $Na_2U_2O_7$(cr) [4] and the mono-hydrated phase investigated in the present work is –232 kJ/mol, a value close to the free energy of formation of water, $\Delta_f G_m^\circ = -(237.14 \pm 0.04)$ kJ/mol. This is roughly consistent with the release in solution of one additional water molecule in the dissolution reaction of $Na_2U_2O_7 \cdot H_2O$(cr), compared to the anhydrous material. The corresponding solubility constants of the two phases are $\log {}^*K_{s,0}^\circ$ {$Na_2U_2O_7 \cdot H_2O$(cr), p.w.} = 11.7 and $\log {}^*K_{s,0}^\circ$ {$Na_2U_2O_7$(cr)} = 11.3 [4, 40]. The two values are similar within the same magnitude, with the highly crystalline anhydrous material holding a slightly lower solubility constant than the hydrated solid investigated in the present work. This difference indicates that the Gibbs energy contribution of the structural water molecule in the hydrated $Na_2U_2O_7 \cdot H_2O$(cr) is similar to that of the free liquid water, as already suggested by the NEA-TDB reviewers [4]. Similarly, the difference between $\Delta_f H_m^\circ$ of the hydrated $Na_2U_2O_7 \cdot H_2O$(cr) in the present work, and that of the selected anhydrous $Na_2U_2O_7$(cr), –(285.8 kJ/mol), is consistent with the enthalpy of formation of a molecule of water –(237.14 ± 0.04) kJ/mol. The difference between these to values (–285.8 + 237.14) yields a net contribution of –39 kJ/mol that we attribute to the formal hydration of the anhydrous material (7) as discussed above.

3.3.4 Solubility and hydrolysis model at $T = 55$, 80 °C

The solubility data of $UO_3 \cdot 2H_2O$(cr) in the acidic range determined at $T = 55$ and 80 °C show a similar trend with respect of the one at $T = 25$ °C. Although this may suggest that the solubility at the different temperatures is controlled by analogous hydrolysis equilibria, the observed alteration of the initial solid phase (see Section 3.2) prevents deriving a conclusive solubility model for this pH_m-region and temperature range. The lack of precise solubility data about $Na_2U_2O_7 \cdot H_2O$(cr) under moderately alkaline pH_m-conditions where the hydrolysis species $UO_2(OH)_3^-$ prevails prevents also to gain insight in the temperature dependence of the corresponding hydrolysis constant.

The solubility constants of $Na_2U_2O_7 \cdot H_2O$(cr) ($\log {}^*K_{s,0}^\circ$, $I = 0$, $T = 55$, 80 °C, (8) Table 1) were calculated from $\log {}^*K_{s,0}^\circ$ at $T = 25$ °C and the values of ΔH_s° (8) at $T = 55$, 80 °C. The enthalpy values were estimated from the values $\Delta^*H_s^\circ(T)$ (4), calculated as explained above, and the enthalpies for the formation of water taken from the CODATA reference values (see Table 1) [34].

$$0.5Na_2U_2O_7 \cdot H_2O(cr) + H_2O(l) = Na^+ + UO_2^{2+} + 3OH^- \quad (8)$$

The resulting trend of ΔH_s° vs. T according to (9) shows a good linearity ($r_{fit}^2 > 0.995$, Figure 5). $\Delta^* H_s^\circ(T)$ shows, instead, a non-linear dependence with the temperature. This is due, in turn, to the non-linear temperature dependence of the enthalpy of protolysis of water itself (Table 1). Therefore, a plot of $\Delta^* H_s^\circ(T)$ vs. T would not have been suitable for the purposes of this calculation.

$$\Delta H_s^\circ(T) = \Delta H_s^\circ(T = 0\ K) + C_{p,m} \cdot T \quad (9)$$

The linear regression (solid line) of the experimental ΔH_s° values at $T = 25$, 45 and 80 °C yields $\Delta H_s^\circ(T = 0\ K) = (237.8 \pm 5.4)$ kJ mol^{-1} and $C_{p,m} = -(0.463 \pm 0.017)$ kJ K^{-1} mol^{-1}. The temperature dependence of the heat capacity $C_{p,m}$ can be therefore neglected ($dC_{p,m}/dT \approx 0$). Accordingly, log $^*K_{s,0}^\circ$ values at $T = 55$ and 80 °C were calculated with the formula in (10) and are summarized in Table 1.

$$\log K_s^\circ(T) = \log K_s^\circ(298.15\,K) + \frac{\Delta H_s^\circ(298.15\,K)}{R \ln 10}\left(\frac{1}{298.15} - \frac{1}{T}\right) + \frac{C_{p,m}}{R \ln 10}\left(\frac{298.15}{T} - 1 + \ln\left(\frac{T}{298.15}\right)\right) \quad (10)$$

The sets of solubility data (log [U(VI)] vs. T) in the alkaline range at $T = 55$ and 80 °C [Table S2 as supplementary information) were independently analyzed with a least-square minimization process to calculate the values of the hydrolysis constants of $UO_2(OH)_4^{2-}$ ($\log {}^*\beta_{1,4}^\circ$, $I = 0$, $T = 55$, 80 °C, (11)).

$$UO_2^{2+} + 4H_2O(l) = UO_2(OH)_4^{2-} + 4H^+ \quad (11)$$

The calculated values resulted in $\log {}^*\beta_{1,4}^\circ = -(29.7 \pm 0.2)$ and $-(28.3 \pm 0.2)$ at $T = 55$ and 80 °C, respectively. The speciation model used in the calculation includes the values of $\log {}^*K_{s,0}^\circ$ at $T = 55$ and 80 °C estimated as indicated above. The SIT parameters of the different ionic species at $T = 25$ °C were presumed to have the same value at $T = 55$ and 80 °C. In general this is a good approximation, since the temperature dependence of the SIT interaction parameters in the temperature range $T = 0$–100 °C can be neglected in most cases (in the order of 10^{-3} kg mol^{-1} K^{-1}, as seen above in the case of the calorimetric data in $HClO_4$ medium) [39]. A numerical analysis of the data including an optimization of the SIT parameter ε(Na^+, $UO_2(OH)_4^{2-}$) was attempted, but the quality of the fit did not improve significantly enough to justify such optimization.

A value of the molar enthalpy of (11), $\Delta^* H_{1,4}^\circ = (134 \pm 7)$ kJ/mol was estimated from the linear regression of $\log {}^*\beta_{1,4}^\circ$ vs. $1/T$ and assuming $d\Delta^* H_{1,4}^\circ / dT = 0$ (Van't Hoff approach, see Figure 6) [37].

Determinations of the value of $\Delta^* H_{1,4}^\circ$ from experimental data are very scarce in the literature and no value has been selected so far by the NEA-TDB [4]. In fact, as evidenced by the present work, the study of the hydrolysis of U(VI) in the alkaline range is hampered by several factors. First, the relatively low solubility of uranium itself ([U(VI)] < 10^{-5} m) is often below the detection limit of most spectroscopic and calorimetric techniques. In addition, since $UO_2(OH)_4^{2-}$ forms only in alkaline and hyperalkaline conditions ($pH_m > 11.5$), the use of titration potentiometry to investigate this system is limited. Recently, Di Bernardo et al. [10] reported an experimentally determined value of $\Delta^* H_{1,4}^\circ = (167.6 \pm 1.7)$ kJ/mol (3 σ uncertainty). In this

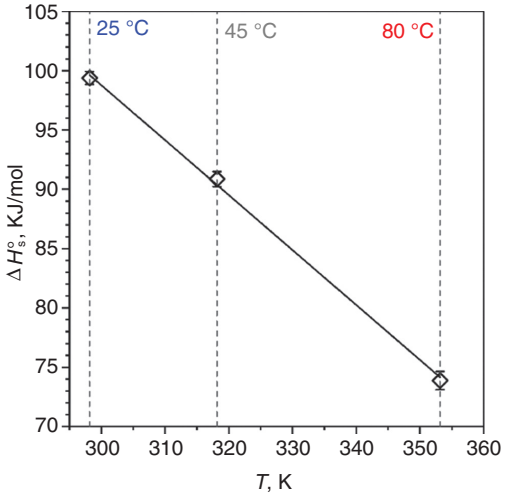

Figure 5: Linear regression of ΔH_s° vs. T for (9) according with $\Delta H_s^\circ = \Delta H_s^\circ(T = 0\,K) + C_{p,m} \cdot T$.

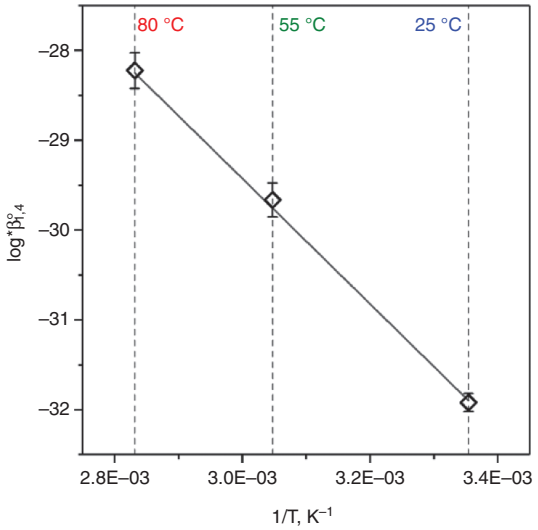

Figure 6: Van't Hoff plot of $\log {}^*\beta_{1,4}^\circ$ vs. $1/T$.

study, titration microcalorimetry was used to investigate the hydrolysis and peroxide formation equilibria of UO_2^{2+} in acidic and alkaline solutions of 0.1 M $(CH_3)_3N(NO_3)$ at $T = 25$ °C. This particular background electrolyte was likely chosen to avoid the precipitation of the sparingly soluble $Na_2U_2O_7 \cdot H_2O(cr)$ phase. The enthalpy value determined in this work and the one from Di Bernardo and co-workers differ by ~34 kJ/mol. The two values are still in reasonable agreement, considering the different experimental conditions used, and the abovementioned experimental difficulties involved in the study of this system in these conditions. We consider the value of $\Delta^* H^\circ_{1,4}$ obtained in the present work to be a reliable estimate, since it was determined from solubility data collected at the thermodynamic solid/solution equilibrium and solution calorimetric data of the same solid phase at different temperatures. The enthalpy value currently determined is also corroborated by the U(VI) solubility data previously reported [15]. In our previous study, the calculated values of $\log {}^* K^\circ_{s,(1,4)}$ corresponding to the solubility equilibrium (12) were $\log {}^* K^\circ_{s,(1,4)} = -(20.1 \pm 0.3)$ and $-(18.0 \pm 0.1)$ (2σ uncertainty) at $T = 22$ and 80 °C, respectively. Using the Van't Hoff relation, a value of $\Delta^* H^\circ_{s,(1,4)} = (72 \pm 4)$ kJ/mol for (12) was calculated.

$$0.5\ Na_2U_2O_7 \cdot H_2O(cr) + 2H_2O(l) = Na^+ + UO_2(OH)_4^{2-} + H^+ \quad (12)$$

The corresponding values calculated in the present work are $\log {}^* K^\circ_{s,(1,4)} = -(20.2 \pm 0.3)$ and $-(18.3 \pm 0.4)$ (2σ uncertainty) at $T = 25$ and 80 °C, respectively. These values are in very good agreement with the previous ones determined. The calculated enthalpy value, $\Delta^* H^\circ_{s,(1,4)} = (71 \pm 3)$ kJ/mol (12) is also in excellent agreement.

4 Conclusions

The solubility of $UO_3 \cdot 2H_2O(cr)$ and $Na_2U_2O_7 \cdot H_2O(cr)$ was investigated in 0.10, 0.51 and 5.6 m NaCl solutions with $4 \le pH_m \le 14.3$ at $T = 25$, 55 and 80 °C. The enthalpy of dissolution of $Na_2U_2O_7 \cdot H_2O(cr)$ at $T = 25$, 45 and 80 °C was independently determined by means of solution-drop calorimetry. An extensive characterization of the solid materials before and after the completion of the solubility experiments was conducted. Results from the different experimental approaches allow evaluating the impact of temperature and of the ionic medium on the solubility of the different solids, the stability of the solid phases and possible structural changes occurring. A solid phase transformation of $UO_3 \cdot 2H_2O(cr)$ into a sodium uranate-like material is observed in acidic solutions with [NaCl] ≥ 0.51 m and $T = 80$ °C. An alteration of the solid phase is not observed in experiments conducted at $T = 25$ °C.

The calculated value of the solubility constant of $UO_3 \cdot 2H_2O(cr)$ at $T = 25$ °C is $\log {}^* K^\circ_{s,0} = (5.1 \pm 0.2)$. This value is slightly lower, but in agreement within the respective uncertainties, than $\log {}^* K^\circ_{s,0} = (5.35 \pm 0.13)$ recently determined by Altmaier and co-workers [5] for the same U(VI) solid phase. The small differences between the two solubility constants might be related to the tempering step at $T = 80$ °C used in the present study (and absent in Altmaier et al.), that may have induced a slight increase of crystallinity of $UO_3 \cdot 2H_2O(cr)$ in the present work.

$Na_2U_2O_7 \cdot H_2O(cr)$ is the thermodynamically stable solid phase in the alkaline NaCl solutions investigated at $T = 25$, 55 and 80 °C. The solubility data of $Na_2U_2O_7 \cdot H_2O(cr)$, together with the dissolution heat of $Na_2U_2O_7 \cdot H_2O(cr)$ determined by solution calorimetry were used to derive a thermodynamic model for the solubility and hydrolysis behavior of $Na_2U_2O_7 \cdot H_2O(cr)$ in alkaline and hyperalkaline pH_m conditions. In this pH_m-region, the solubility is governed by the formation of $UO_2(OH)_4^{2-}$ and it is significantly enhanced (up to 2.5 $\log_{10}$-units) by temperature compared to the solubility of the same solid phase analyzed at 25 °C. This effect is mainly attributed to the known increased acidity of water at elevated temperatures. The temperature dependence of the solubility product $Na_2U_2O_7 \cdot H_2O(cr)$ and of the hydrolysis constant of $UO_2(OH)_4^{2-}$ also suggest that minor contributions additionally result from a decreased stability of $Na_2U_2O_7 \cdot H_2O(cr)$, together with an enhanced stabilization of $UO_2(OH)_4^{2-}$ with increasing temperature. From the values of $\log {}^* \beta^\circ_{1,4}$ at different temperatures, the reaction enthalpy for the formation of $UO_2(OH)_4^{2-}$ ($\Delta^* H^\circ_{1,4}$) was determined. These results extend our previous thermodynamic studies and allow accurate solubility and speciation calculations for U(VI) in dilute to concentrated, alkaline NaCl solutions in the temperature range $T = 25$–80 °C.

The combination of solubility experiments at elevated temperatures with the calorimetric characterization of the solid phase/s controlling the solubility opens new perspectives in the thermodynamic description of radionuclide aqueous systems of relevance in the context of HLW disposal. In the framework of the German collaborative project ThermAc, these results contribute to the experimental validation of the methods developed for the systematic estimation of thermodynamic properties and temperature dependence of radionuclide aqueous species and solid compounds.

Acknowledgments: The authors would like to thank F. Geyer, C. Walschburger, M. Böttle, S. Heck, S. Moisei-Rabung, T. Kisely and E. Soballa (KIT–INE) for their lab assistance and ICP–MS, ICP–OES, TG–DTA, TOC and SEM–EDS analyses. This work was partially funded by the German Federal Ministry for Education and Research (BMBF). KIT–INE is working in ThermAc under the contract 02NUK039A. The calorimetric experiments were supported by the Director, Office of Science, Office of Basic Energy Science of the US Department of Energy, under Contract No. DE-AC02-05CH11231 at Lawrence Berkeley National Laboratory.

References

1. Wronkiewicz, D. J., Buck, E. C.: Uranium mineralogy and the geologic disposal of spent nuclear fuel. Rev. Mineral. **38**, 475 (1999).
2. Metz, V., Geckeis, H., Gonzalez-Robles, E., Loida, A., Bube, C., Kienzler, B.: Radionuclide behaviour in the near-field of a geological repository for spent nuclear fuel. Radiochim. Acta **100**, 699 (2012).
3. Torrero, M. E., Casas, I., de Pablo, J., Sandino, M. C. A., Grambow, B.: A comparison between unirradiated UO2(s) and schoepite solubilities in 1 M NaCl medium. Radiochim. Acta **66/67**, 29 (1994).
4. Guillamont, R., Fanghänel, T., Neck, V., Fuger, J., Palmer, D. A., Grenthe, I., Rand, M.: Update on the Chemical Thermodynamics of Uranium, Neptunium, Plutonium, Americium and Technetium. OECD Nuclear Energy Agency, Thermodynamic Data Bank, Issy-les-Moulineaux, France (2003), p. 964.
5. Altmaier, M., Yalçıntaş, E., Gaona, X., Neck, V., Müller, R., Schlieker, M., Fanghänel, T.: Solubility of U(VI) in chloride solutions. I. The stable oxides/hydroxides in NaCl systems, solubility products, hydrolysis constants and SIT coefficients. J. Chem. Thermodyn. **114**, 2 (2017).
6. Çevirim-Papaioannou, N., Yalçıntaş, E., Gaona, X., Dardenne, K., Altmaier, M., Geckeis, H. Redox chemistry of uranium in reducing, dilute to concentrated NaCl solutions. Appl. Geochemistry **98**, 286 (2018).
7. Cevirim Papaioannou, E., Yalcintas, E., Gaona, X., Altmaier, M., Geckeis, H.: Solubility of U(VI) in chloride solutions. II. The stable oxides/hydroxides in alkaline KCl solutions: thermodynamic description and relevance in cementitious systems. Appl. Geochem. **98**, 237 (2018).
8. Rao, L., Srinivasan, T. G., Garnov, A. Y., Zanonato, P., Di Plinio, B., Bismondo, A.: Hydrolysis of neptunium(V) at variable temperatures (10-85 °C). Geochim. Cosmochim. Acta **68**, 4821 (2004).
9. Zanonato, P. L., Di Bernardo, P., Bismondo, A., Liu, G., Chen, X., Rao, L.: Hydrolysis of uranium(VI) at variable temperatures (10–85 °C). J. Am. Chem. Soc. **126**, 5515 (2004).
10. Zanonato, P. L., Di Bernardo, P., Grenthe, I.: A calorimetric study of the hydrolysis and peroxide complex formation of the uranyl(VI) ion. Dalt. Trans. **43**, 2378 (2014).
11. Zanonato, P. L., Di Bernardo, P., Zhang, Z., Gong, Y., Tian, G., Gibson, J. K., Rao, L.: Hydrolysis of thorium(IV) at variable temperatures. Dalt. Trans. **45**, 12763 (2016).
12. Hála, J., Miyamoto, H.: IUPAC-NIST Solubility Data Series. 84. Solubility of inorganic actinide compounds. J. Phys. Chem. Ref. Data **36**, 1417 (2007).
13. Brown, P. L., Ekberg, C.: Hydrolysis of metal ions. Wiley-VCH, Verlag GmbH & Co. KGaA, Weinheim (2016), p. 917.
14. Ciavatta, L.: The specific interaction theory in evaluating ionic equilibriums. Ann. Chim. **70**, 551 (1980).
15. Endrizzi, F., Gaona, X., Marques Fernandes, M., Baeyens, B., Altmaier, M.: Solubility and hydrolysis of U(VI) in 0.5 mol/kg NaCl solutions at T = 22 and 80 °C. J. Chem. Thermodyn. **120**, 45 (2018).
16. Nikitin, A. A., Sergeeva, E. I., Khodakovskii, I. L., Naumov, G. B.: Hydrolysis of Uranyl in the hydrothermal region. Geokhimiya **3**, 297 (1972).
17. Nikolaeva, N. M., Pirozhkov, A. V.: Determination of the solubility product of uranyl hydroxide at elevated temperatures. Izv. Sib. Otd. Akad. Nauk SSSR, Seriya Khimicheskikh Nauk. **4**, 73 (1971).
18. Lemire, R. J., Tremaine, P. R.: Uranium and plutonium equilibriums in aqueous solutions to 200 °C. J. Chem. Eng. Data. **25**, 361 (1980).
19. Valsami-Jones, E., Ragnarsdottir, K. V.: Solubility of uranium oxide and calcium uranate in water and Ca(OH)2-bearing solutions. Radiochim. Acta **79**, 249 (1997).
20. Arocas, P. D., Grambow, B.: Solid-liquid phase equilibria of U(VI) in NaCl solutions. Geochim. Cosmochim. Acta **62**, 245 (1998).
21. Gorman-Lewis, D., Fein, J. B., Burns, P. C., Szymanowski, J. E. S., Converse, J.: Solubility measurements of the uranyl oxide hydrate phases metaschoepite, compreignacite, Na-compreignacite, becquerelite, and clarkeite. J. Chem. Thermodyn. **40**, 980 (2008).
22. Debets, P. C., Loopstra, B. O.: The uranates of ammonium. II. X-ray investigation of the compounds in the system NH3-UO3-H2O. J. Inorg. Nucl. Chem. **25**, 945 (1963).
23. Finch, R. J., Ewing, R. C.: Clarkeite: new chemical and structural data. Am. Mineral. **82**, 607 (1997).
24. Rabinowitch, E., Belford, R. L.: International Series of Monographs on Nuclear Energy, Chemistry Division. Vol. 1. Spectroscopy and Photochemistry of Uranyl Compounds. New York Macmillan (1964), p. 300.
25. Gorobets, B. S., Sidorenko, G. A.: Luminescence of secondary uranium minerals at low temperatures. At. Energiya. **36**, 6 (1974).
26. Parker, V. B.: Thermal Properties of Aqueous Uni-univalent Electrolytes. US National Bureau of Standards (1965), p. 76.
27. Kuznetsov, L. M., Tsvigunov, A. N.: Hydrothermal synthesis and physicochemical study of sodium triuranate monohydrate (Na2U3O10.H2O). Radiokhimiya **22**, 600 (1980).
28. Wang, Z., Zachara, J. M., Gassman, P. L., Liu, C., Qafoku, O., Yantasee, W., Catalano, J. G.: Fluorescence spectroscopy of U(VI)-silicates and U(VI)-contaminated Hanford sediment. Geochim. Cosmochim. Acta **69**, 1391 (2005).
29. Wang, Z., Zachara, J. M., Liu, C., Gassman, P. L., Felmy, A. R., Clark, S. B.: A cryogenic fluorescence spectroscopic study of uranyl carbonate, phosphate and oxyhydroxide minerals. Radiochim. Acta **96**, 591 (2008).

30. Gorobets, B. S., Engoyan, S. S., Sidorenko, G. A.: Study of uranium and uranium-containing minerals using luminescence spectra. At. Energiya. **42**, 177 (1977).
31. Volod'ko, L. V., Komyak, A. I., Sevchenko, A. N., Umreiko, D. S.: Spectral-luminescent study of crystals of uranyl compounds. J. Lumin. **8**, 198 (1974).
32. Brittain, H. G., Perry, D. L.: Luminescence spectra of the uranyl ion in two geometrically similar coordination environments. Uranyl nitrate hexahydrate and di-μ-aquo-bis[dioxobis(nitrato) uranium(VI)] diimidazole. J. Phys. Chem. **84**, 2630 (1980).
33. Baran, V., Tympl, M.: Thermal analysis of sodium uranates. Zeitschrift fuer Anorg. und Allg. Chemie. **347**, 184 (1966).
34. Cox, J. D., Wagman, D. D., Medvedev, V. A.: CODATA Key Values for Thermodynamics. Hemisphere Publ. Corp. (1989), p. 271.
35. Merli, L., Fuger, J.: Thermochemistry of a few neptunium and neodymium oxides and hydroxides. Radiochim. Acta **66/67**, 109 (1994).
36. Zanonato, P. L., Di Bernardo, P., Grenthe, I.: Chemical equilibria in the binary and ternary uranyl(VI)-hydroxide-peroxide systems. Dalton. Trans. **41**, 3380 (2012).
37. Grenthe, I., Puigdomènech, I., Allard, B.: Modelling in Aquatic Chemistry. Nuclear Energy Agency, Organisation for Economic Co-operation and Development 1997.
38. Pitzer, K. S. ed: Activity coefficients in electrolyte solutions. CRC Press, Boca Raton [u.a.] (1991), p. 542 S.
39. Puigdomènech, I., Rard, J. A., Plyasunov, A. V., Grenthe, I.: Temperature Corrections to Thermodynamic Data and Enthalpy Calculations., Le Seine-St. Germain 12, Bd. des Îles F-92130 Issy-les-Moulineaux France 1999, p. 1–96.
40. Grenthe, I., Fuger, J., Konings, R. J. M., Lemire, R. J., Muller, A. B., Nguyen-Trung, C., Wanner, H.: Chemical Thermodynamics of Uranium. OECD Nuclear Energy Agency, Thermodynamic Data Bank, Issy-les-Moulineaux (France) (1992), p. 715.
41. Tso, T. C., Brown, D., Judge, A. I., Holloway, J. H., Fuger, J.: Thermodynamics of the actinide elements. Part 6. The preparation and heats of formation of some sodium uranates(VI). J. Chem. Soc. Dalton. Trans. Inorg. Chem. 1853 (1985). https://pubs.rsc.org/en/content/articlelanding/1985/dt/dt9850001853#!divAbstract.
42. Cordfunke, E. H. P., Loopstra, B. O.: Sodium uranates. Preparation and thermochemical properties. J. Inorg. Nucl. Chem. **33**, 2427 (1971).
43. Smith, A. L., Colle, J. -Y., Raison, P. E., Beneš, O., Konings, R. J. M.: Thermodynamic investigation of Na2U2O7 using Knudsen effusion mass spectrometry and high temperature X-ray diffraction. J. Chem. Thermodyn. **90**, 199 (2015).

Supplementary Material: The online version of this article offers supplementary material (https://doi.org/10.1515/ract-2018-3056).